

7th MEETING OF THE SCIENTIFIC COMMITTEE

La Havana, Cuba, 7 to 12 October 2019

SC7-SQ07

Using a size-structure model to assess the Jumbo flying squid in the
equatorial waters

China

Using a size-structured model to assess the jumbo flying squid stock in the equatorial waters

Luoliang xu, Gang Li, Jiaqi Wang, Xinjun Chen, Yong Chen

National Data Center for Distant-water Fisheries, Shanghai Ocean University and University of Maine

1. Introduction:

Jumbo flying squid, *Dosidicus gigas* (d'Orbigny 1835), is widely distributed in the eastern Pacific Ocean (Nigmatullin et al., 2001). Its resource in the South Pacific supports the world largest squid fishery. The catch has surpassed one million metric tons in 2014, which is the highest yield in history (FAO, Figure1).

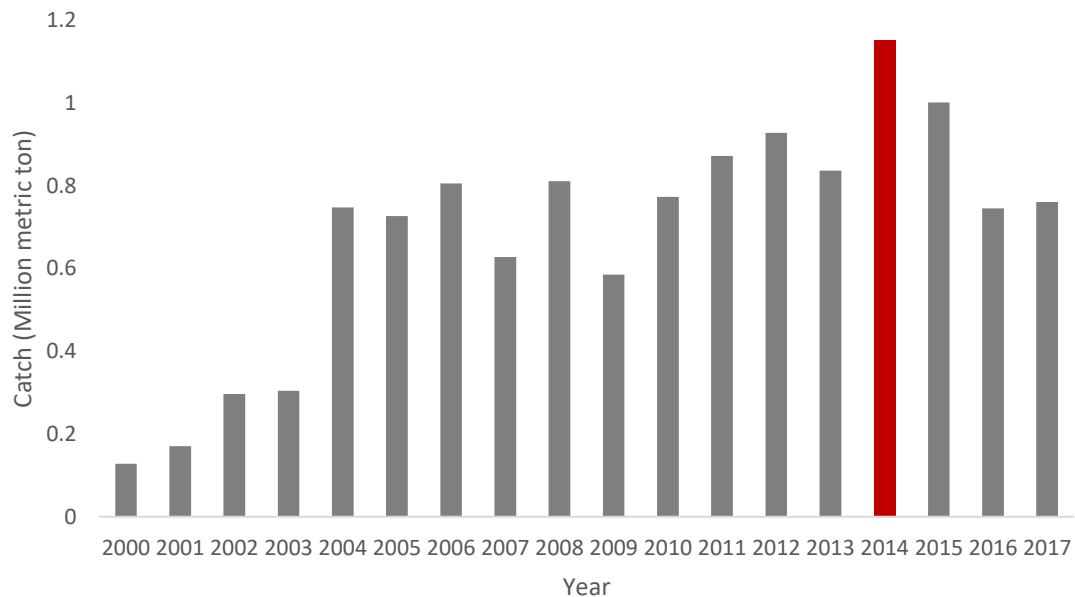


Figure 1. The global catch of jumbo flying squid in South Pacific from year 2000~2017

Three phenotypic groups of jumbo flying squid in South Pacific has been identified by the distinguishable sizes at which individuals reach maturity (Nigmatullin et al., 2001). However, no relevant genetic differences have been found between the three phenotypic groups (Sandoval-Castellanos et al., 2010). It was found that the ambient temperature was important in determining whether a given jumbo flying squid would have early maturation with a small size or delayed maturation with a large size (Arkhipkin et al., 2015). Only small size jumbo flying squid occurs in fishing grounds near the equator with relatively high sea surface temperature (Chen et al., 2013; Figure 2 and 3). Here, we applied a size-structured model to assess the jumbo flying squid in the equatorial waters. One major assumption (not validated or invalidated

yet) of this study is that the jumbo flying squid in this area is a unique stock without emigration to and immigration from other areas.

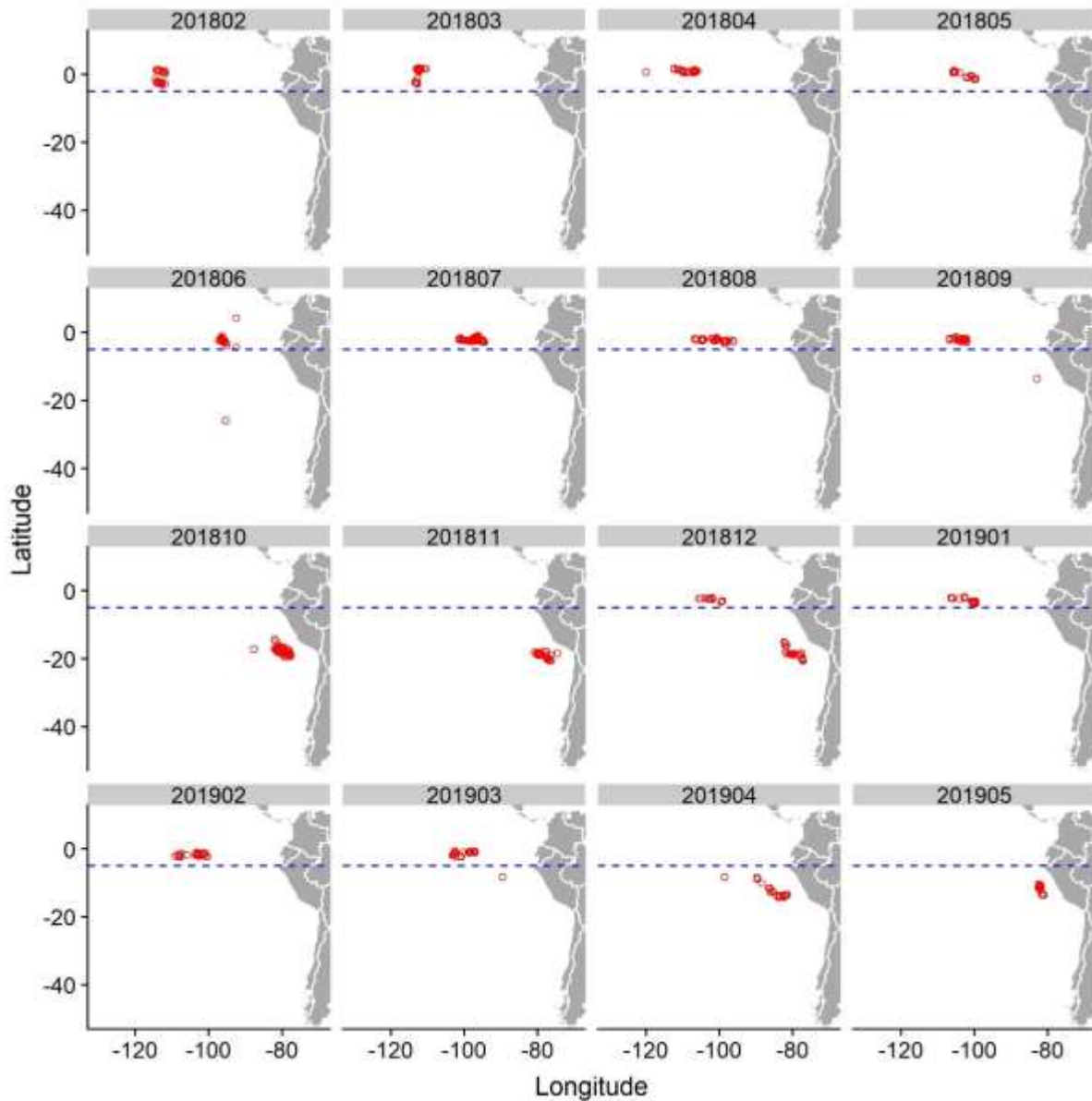


Figure 2. The sample locations of the jumbo flying squid from February 2018 to May 2019. The dashed horizontal line represents 5° S longitude line, which divides the equator fishing ground from Peruvian high sea fishing ground

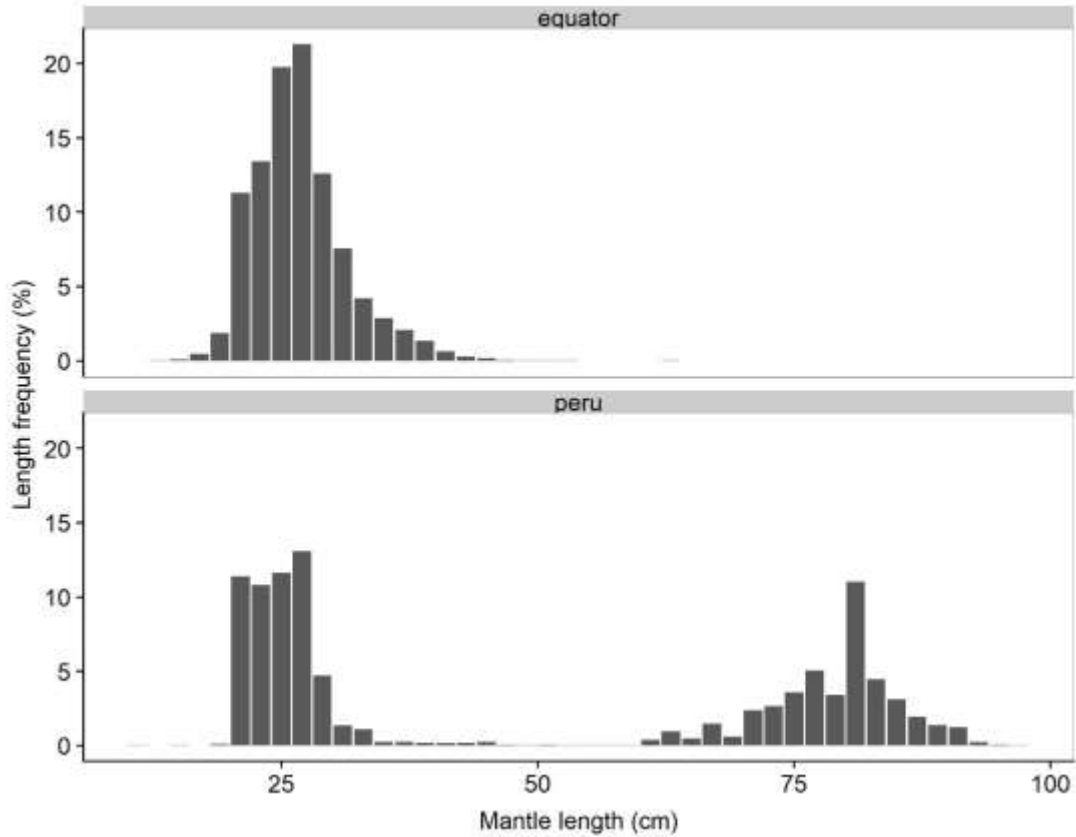


Figure 3. The length frequency of the jumbo flying squid catches in the equator fishing ground (upper panel) and in Peruvian high sea fishing ground (lower panel). Data were collected by an onboard observer and information boats from February 2018 to May 2019

2.Data and methods:

The time series of the stock assessment is from February 2018 to September 2018. The area is limited to the area north of 5° S. The time step of the stock assessment model is month. The technical details of the size-structured model have been presented in the SPRFMO SC meeting in the previous year (SPRFMO SC6-SQ06).

The length composition data were collected by onboard observers and the information vessels. The fishery-dependent biomass index data (CPUE) were from Squid jigging technical group of China Distant Water Fisheries Association. The data field consisted of fishing effort, fishing area (0.5° longitude × 0.5° latitude) and yield. The monthly CPUE was calculated as follows:

$$CPUE_m = \text{mean} (catch_{m,i,j}/effort_{m,i,j}) \quad (1)$$

where $catch_{m,i,j}$ and $effort_{m,i,j}$ were the total catch and total fishing effort, respectively, in month m , latitude i and longitude j .

3. Model configuration:

3.1 Base scenario:

Natural mortality:

The weighted natural mortality for jumbo flying squid of size bin k , month m is calculated as:

$$M_{k,m} = w_k M_m \quad (2)$$

where w_k is pre-specified size weighting factor; and M_m is the monthly natural mortality, which is estimated.

The squid will die soon after spawning. Most spawning stock can not survive and contribute the recruitment in the next time step. Therefore, the natural mortality for the spawning stock should be abnormally high. In order to mimic this process, we assign higher values to w_k for squid with larger sizes. We applied a third-order polynomial function to regress the proportion of the fourth maturity stage at given sizes (Figure 4 and 5). The w_k was calculated as follows:

$$Wk = 9 \times 10^{-5} \times k^3 - 0.0072 \times k^2 + 0.196 \times k - 1.7815; k > 27$$

$$Wk = 9 \times 10^{-5} \times 27^3 - 0.0072 \times 27^2 + 0.196 \times 27 - 1.7815; k \leq 27 \quad (3)$$

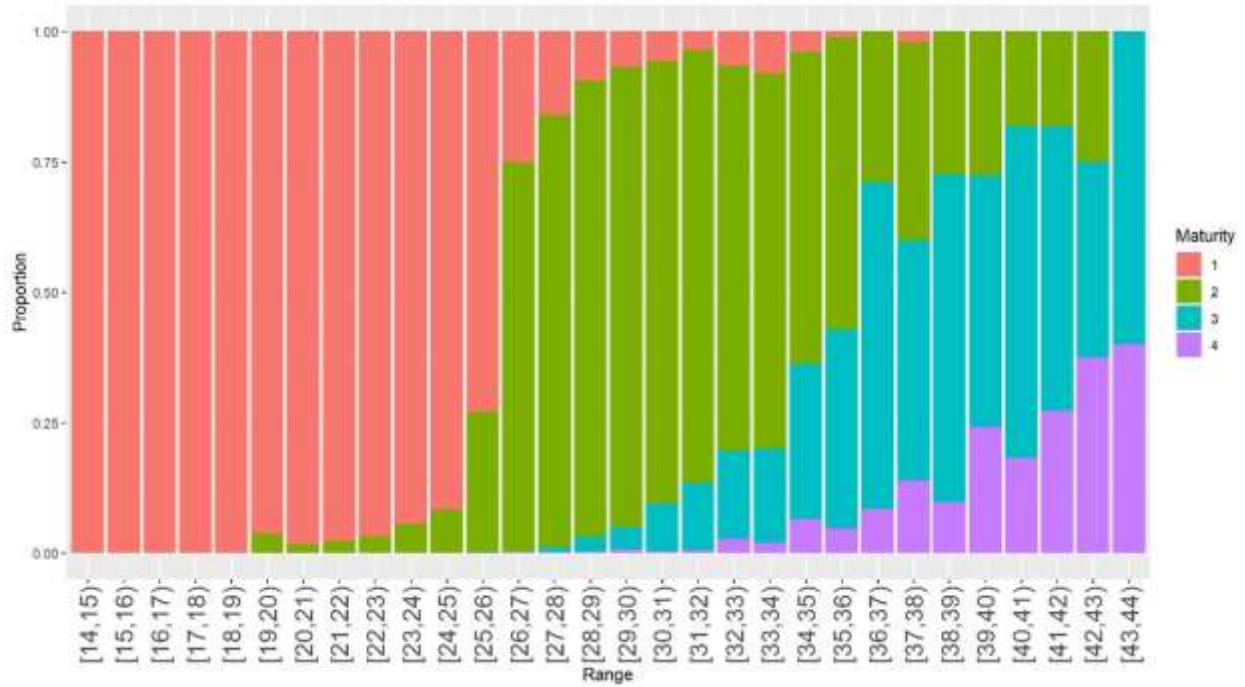


Figure 4. The frequency of the maturity stages of jumbo flying squid in the equator fishing ground

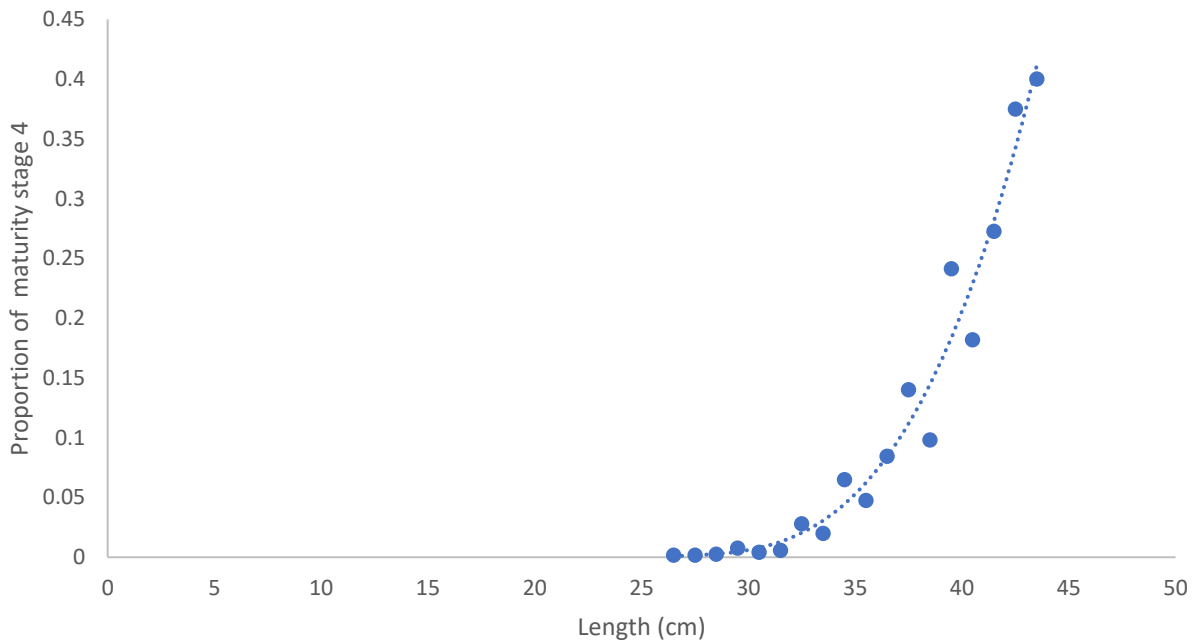


Figure 5. The proportion of the fourth maturity stage at given sizes

Growth matrix:

The growth matrix was constructed externally using the linear growth function and the growth probability function:

$$\text{Length (cm)} = 3.74 * \text{Age (month)} + 3.21 \quad (4) \quad (\text{Liu et al., 2013})$$

$$G_{i,j} = \int_{-\infty}^{L_i + CW} \frac{1}{\sqrt{2\pi}\sigma_j} e^{-\left(\frac{L_i - \bar{L}_j}{2(\sigma_j)^2}\right)^2} dL; \quad L_i = L_{Min}$$

$$G_{i,j} = \int_{L_i}^{L_i + CW} \frac{1}{\sqrt{2\pi}\sigma_j} e^{-\left(\frac{L_i - \bar{L}_j}{2(\sigma_j)^2}\right)^2} dL; \quad L_{Min} < L_i < L_{Max}$$

$$G_{i,j} = \int_{L_i}^{L_i + CW} \frac{1}{\sqrt{2\pi}\sigma_j} e^{-\left(\frac{L_i - \bar{L}_j}{2(\sigma_j)^2}\right)^2} dL; \quad L_i = L_{Max} \quad (5) \quad (\text{Haddon, 2010})$$

where $G_{i,j}$ is the expected probability of growing from size class j into size class i ; σ_j is the standard deviation of the normal distribution of growth increments for size class j ; \bar{L}_j is the expected average size for size class j after the growth expected in one given time interval.

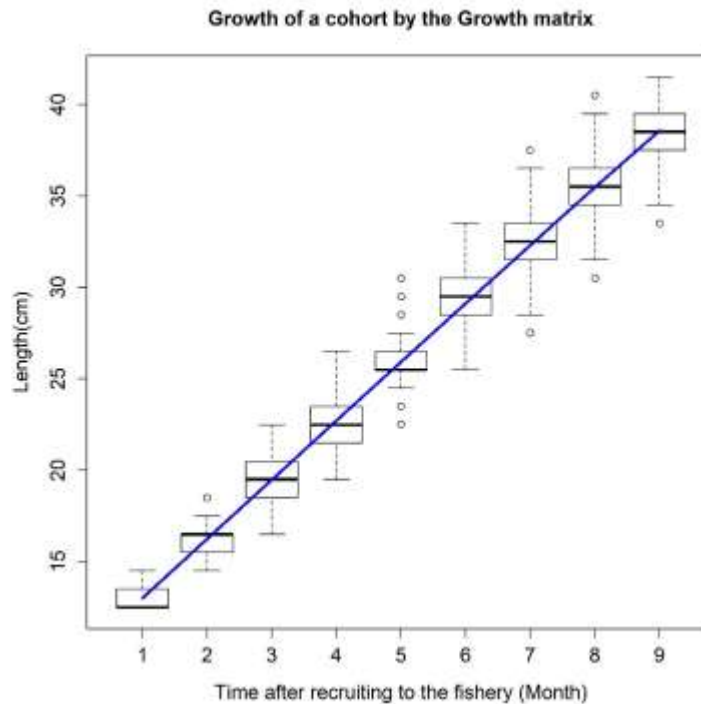


Figure 6. The growth of a cohort of jumbo flying squid

Length-weight relationship:

The length-weight relationship is described as follows:

$$\log(w) = -9.7089 + 2.864 * \log(L) \quad (6) \quad (\text{derived from lab database})$$

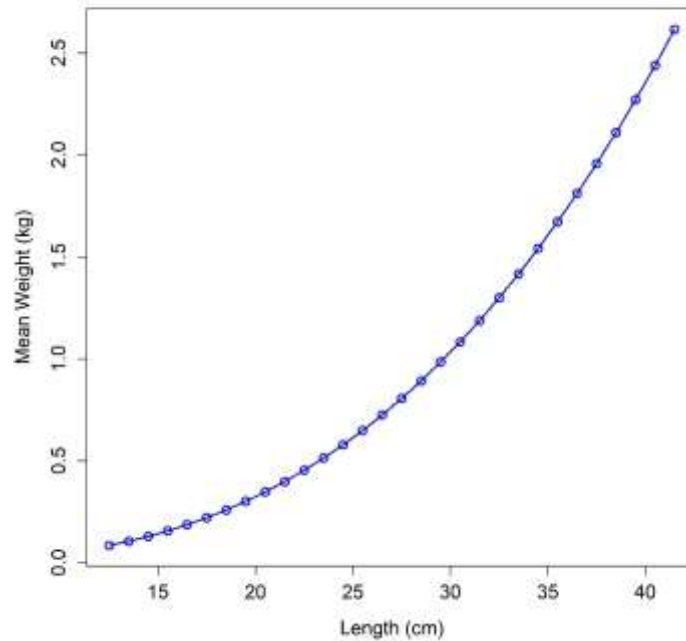


Figure 7. The length-weight relationship of jumbo flying squid

Maturity:

The probability of maturity of a squid in a given size class was calculated by logistic function:

$$p(L) = \frac{1}{1 + e^{-0.4(L-35)}} \quad (7) \quad (\text{derived from lab database})$$

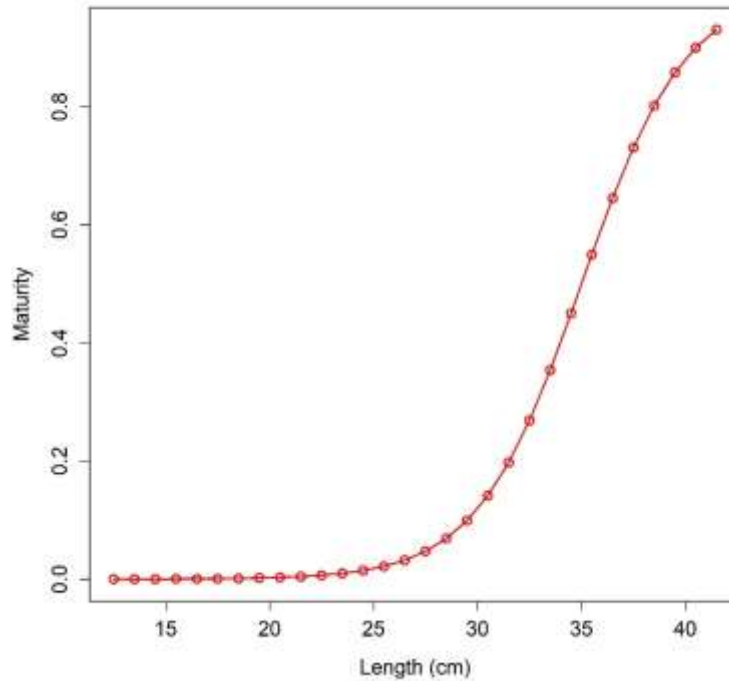


Figure 8. The probability of maturity of jumbo flying squid in given sizes

Recruitment:

There was no function link between the spawning biomass and recruitment in the model. The recruitments for each month were estimated.

Fishing mortality:

The fishing mortality for month m , and size bin k is calculated as a product of month effect F_m and selectivity at the size (S_k):

$$F_{m,k} = F_m S_k \quad (8)$$

the selectivity was calculated by logistic function and the associated parameters (a and b) were estimated in the model:

$$S_k = \frac{1}{1 + \exp(b(a - L_k))} \quad (9)$$

3.2 Sensitivity scenarios:

Sensitivity scenario	Difference from base case	Purpose/Reference
1	Invariable natural mortality for squids with different sizes	Test the impacts of ignoring the high natural mortality associated with semelparity
2	Down weighting the size-composition data	(Francis, 2011)

4.Results:

4.1 Base case

The estimated natural mortality was 0.088 for the squid smaller than 27 cm. The natural mortality increased from 0.088 to 0.962 as the squid length increased from 20 cm to 42 cm. The fishing mortality varied from 0.534 to 0.998 over months. The lowest fishing mortality was in April whereas the highest fishing mortality occurred in August (Figure 9). Estimates of spawning stock biomass ranged from approximately 3,400 metric tons to 6,900 metric tons. The spawning stock biomass decreased from February to April, increased from April to June and then decreased again (Figure 10). The recruitment estimates ranged from 30 billion to 47 billion individuals and peaked in April. The relationship between recruitments and spawning stock biomass was not clear (Figure 11). The goodness of fit of the three types of data (size composition, biomass index, and catch) was shown in Figure 12 and 13.

4.2 Sensitivity scenario 1

The invariable natural mortality was 0.126. The fishing mortality estimates varied over months from 0.689 to 1.286. The fishing mortality estimates were higher than those from base scenario. The fishing selectivity was identical to that from base scenario. The lowest fishing mortality was in May whereas the highest fishing mortality occurred in August (Figure 14). Estimates of spawning stock biomass ranged from approximately 3,100 metric tons to 6,500 metric tons. The spawning stock biomass decreased from February to April, increased from April to June and then decreased again (Figure 15). The trend was similar to the base scenario. The recruitment estimates ranged from 36 billion to 44 billion individuals and peaked in April. The relationship between recruitments and spawning stock biomass was not clear (Figure 16). The goodness of fit of the three types of data (size composition, biomass index, and catch) was shown in Figure 17 and 18.

4.3 Sensitivity scenario 2

The estimated natural mortality was identical to that from base scenario. The fishing mortality estimates varied over months from 0.561 to 1.060. The temporal trend of fishing mortality was similar compared with base scenario and the fishing selectivity was identical to that from base scenario (Figure 19).

Estimates of spawning stock biomass ranged from approximately 3,000 metric tons to 4,500 metric tons. The spawning stock biomass decreased from February to April, increased from April to June and then decreased again (Figure 20). The recruitment estimates ranged from 33 billion to 45 billion individuals, which peaked in April. The relationship between recruitments and spawning stock biomass was not clear (Figure 21). The goodness of fit of size composition data was slightly worse than that of the base scenario and the obvious difference occurred in May, July, and August (Figure 22). The predicted biomass index was much closer with the observed biomass index in this scenario as the size composition data were down-weighted in the objective function (Figure 23).

5.Summary:

It is the first attempt to use a size-structured model to assess the jumbo flying squid in the equatorial waters. The preliminary results have shown the model's potential to parameterize the special biological characteristics of jumbo flying squid (e.g., natural mortality associated with semelparity). The monthly time step seems to be appropriate for modelling the population dynamics of jumbo flying squid, however it requires monthly size composition data hence increases the difficulty of data collection.

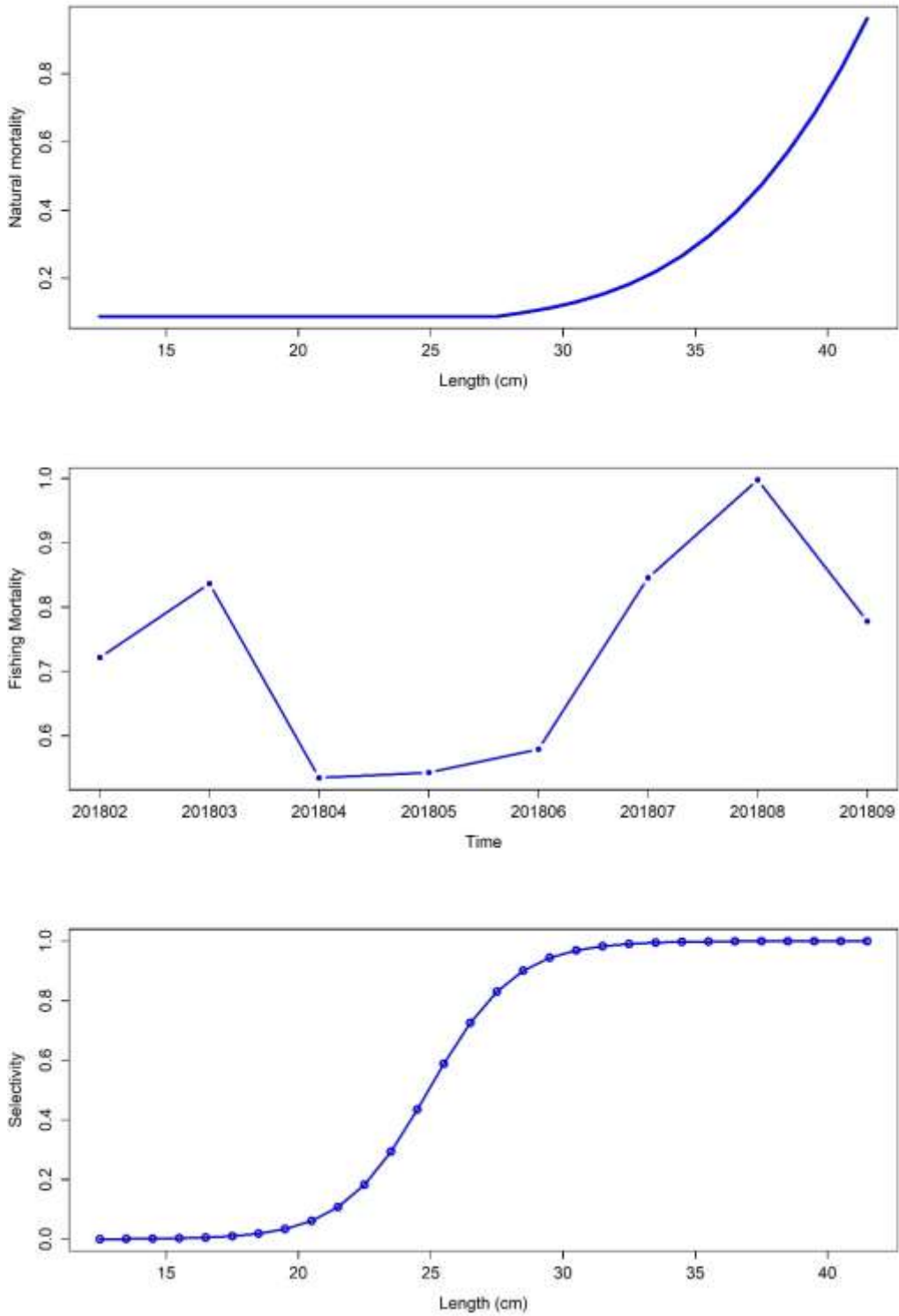


Figure 9. The estimates of natural mortality (upper panel), fishing mortality (middle panel), and selectivity (lower panel) from base scenario

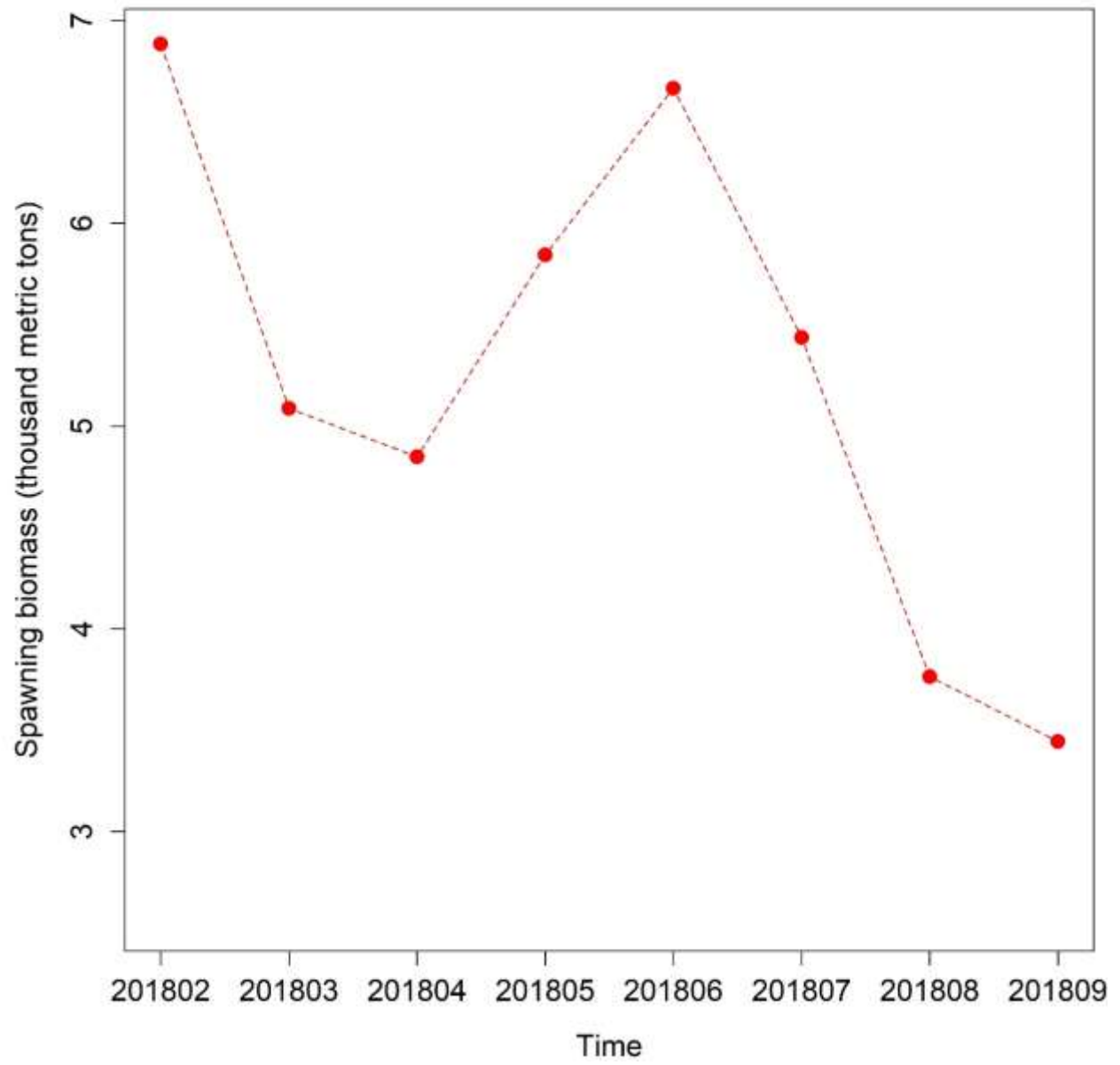


Figure 10. The estimates of spawning biomass from base scenario

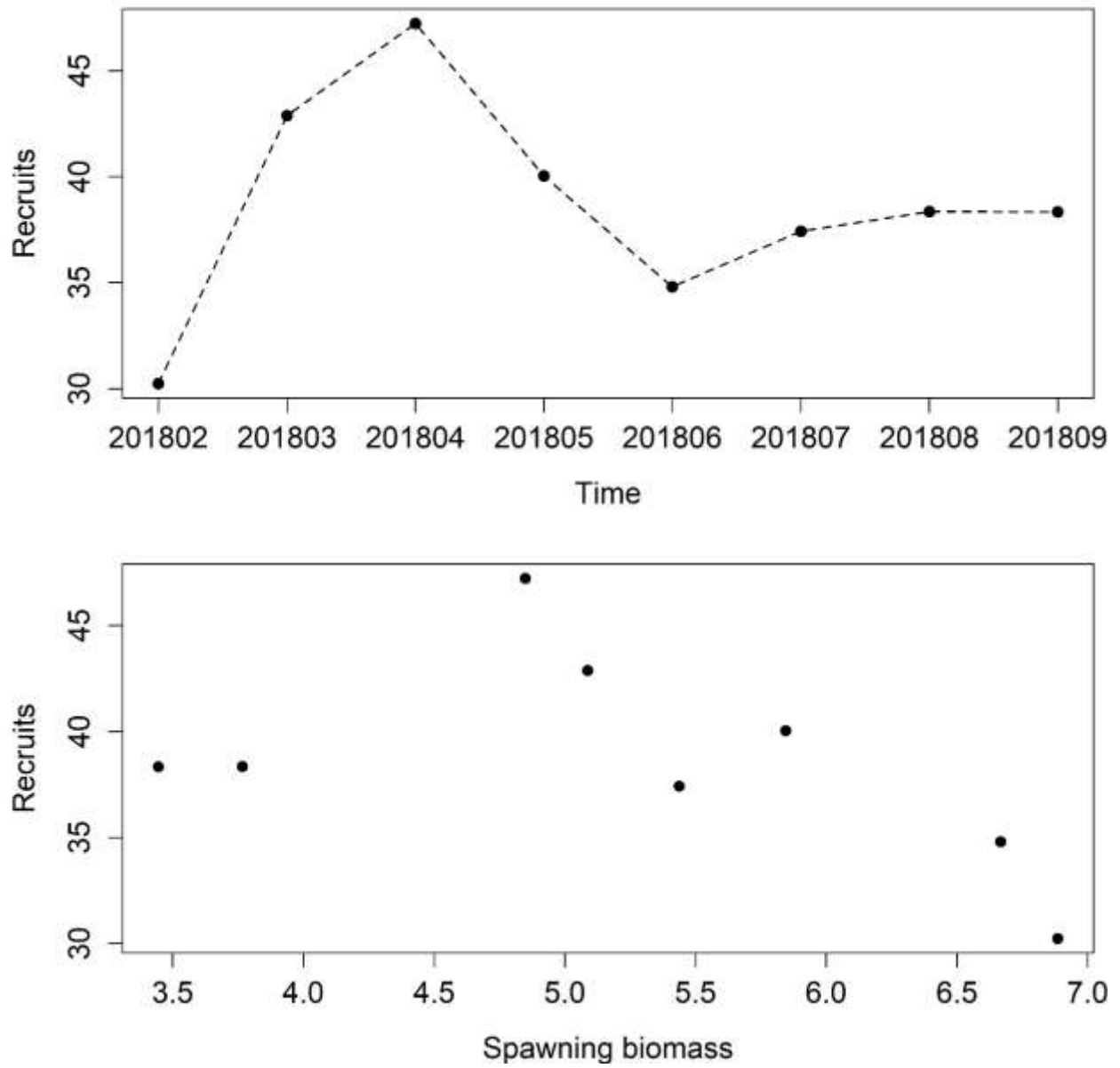


Figure 11. The estimates of recruitments (upper panel) from base scenario and the relationship between spawning biomass and recruitments (lower panel)

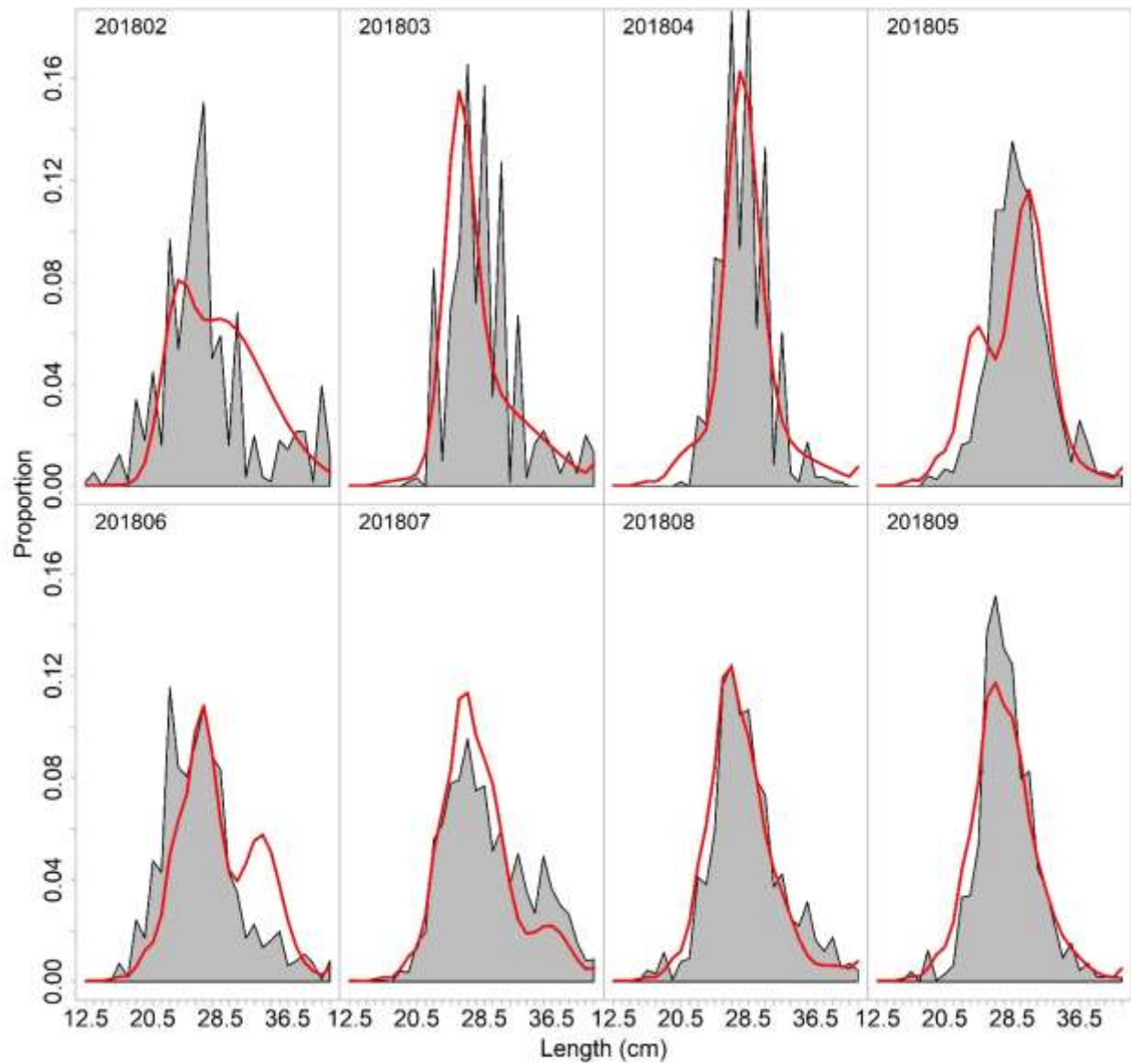


Figure 12. The observed size composition data and the predicted size compositions from base scenario; the red line represents the prediction

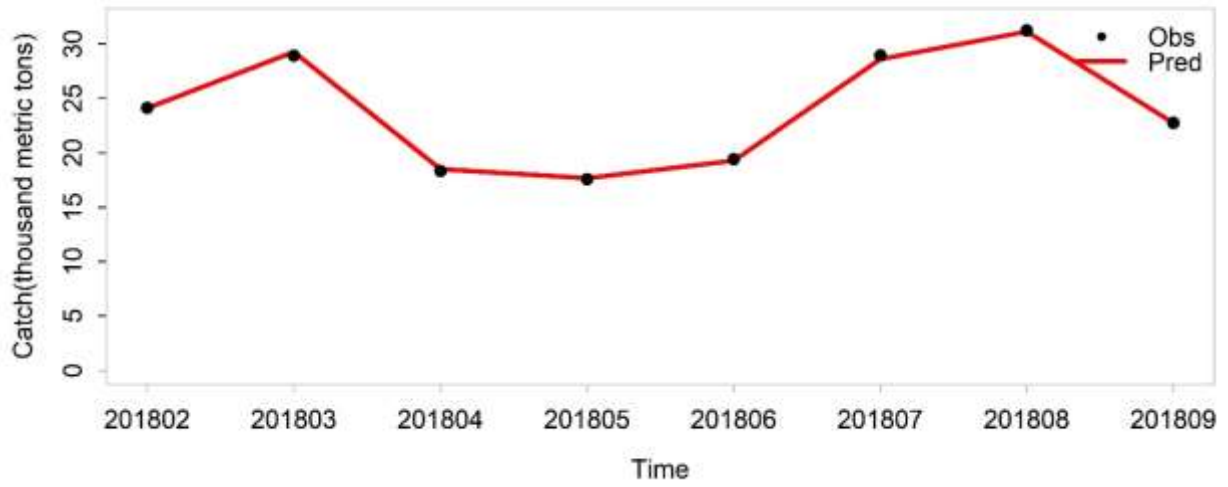
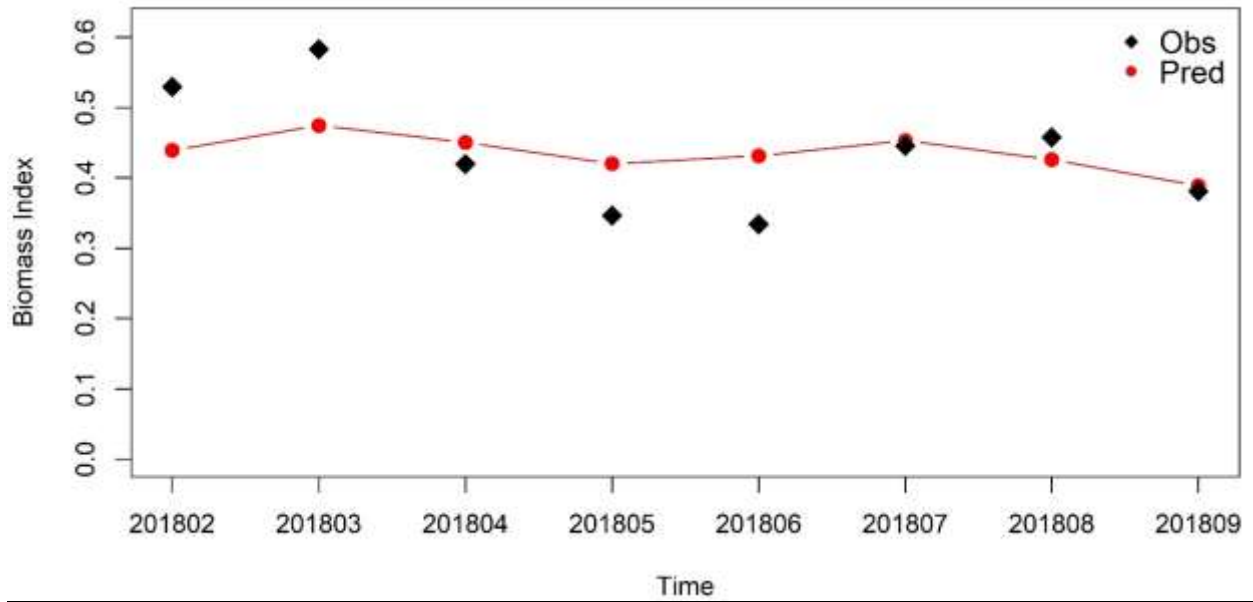


Figure 13. The observed and the predicted biomass index (upper panel) and catch (lower panel); the red line represents the prediction

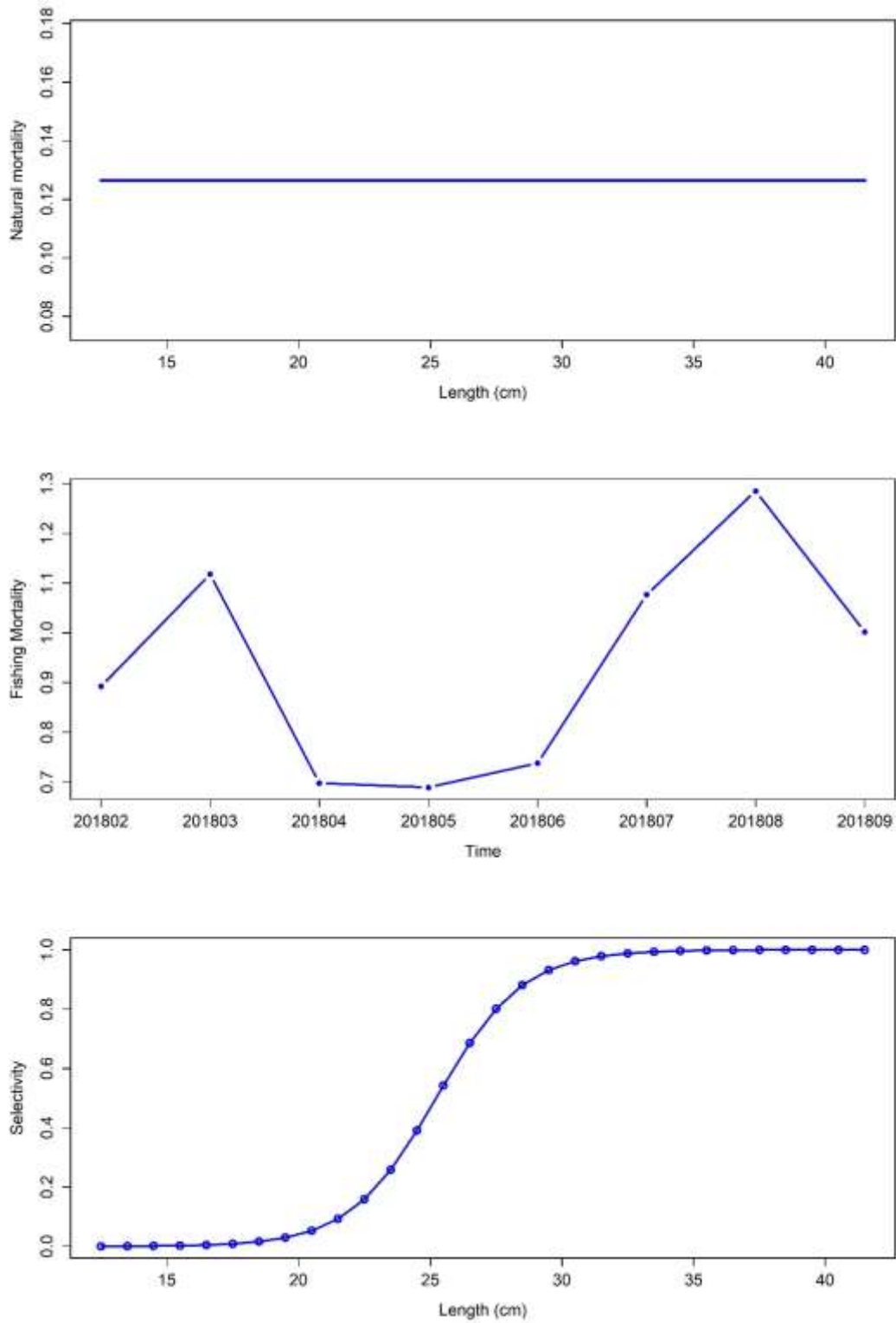


Figure 14. The estimates of natural mortality (upper panel), fishing mortality (middle panel), and selectivity (lower panel) from sensitivity scenario 1

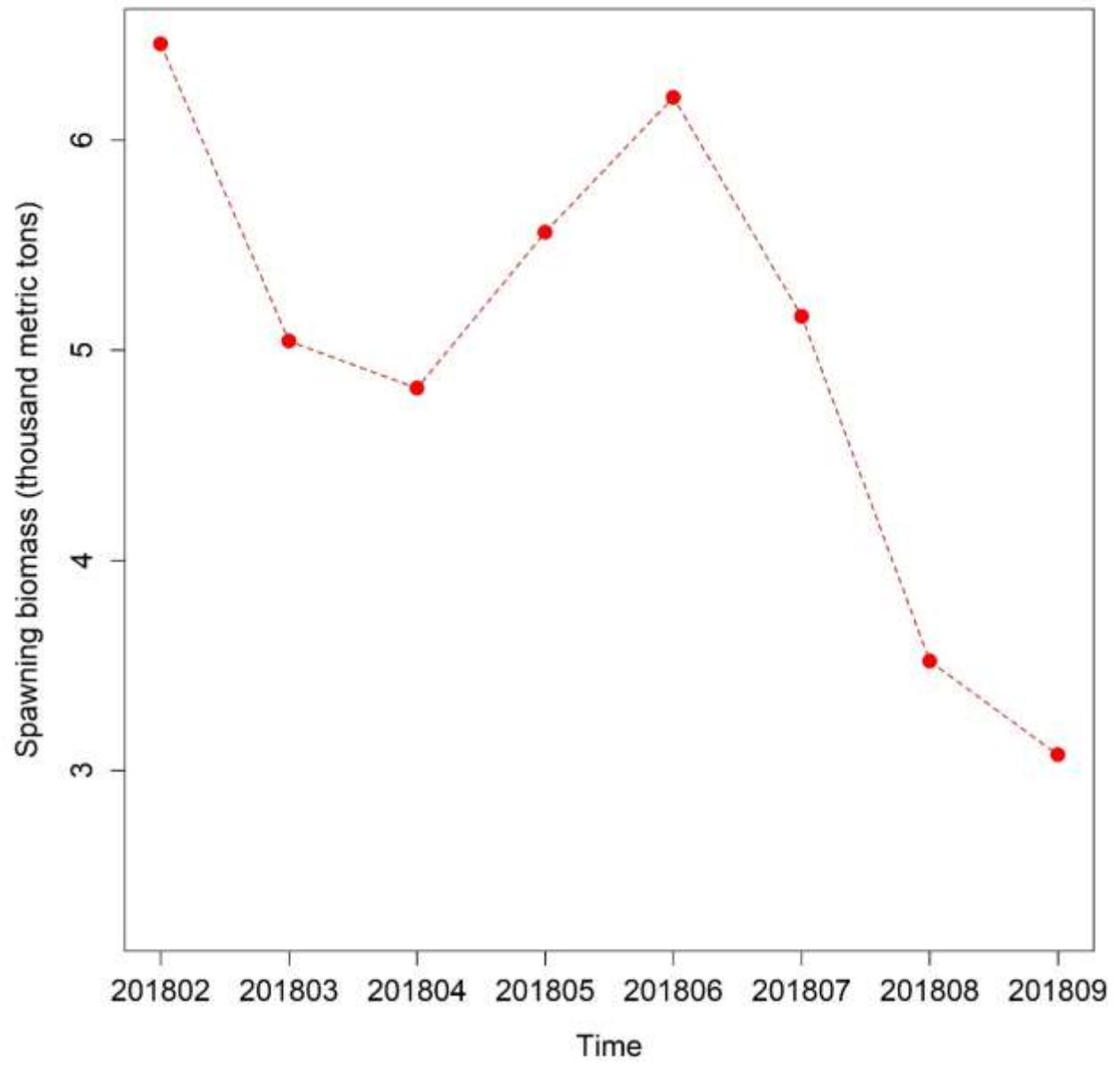


Figure 15. The estimates of spawning biomass from sensitivity scenario 1

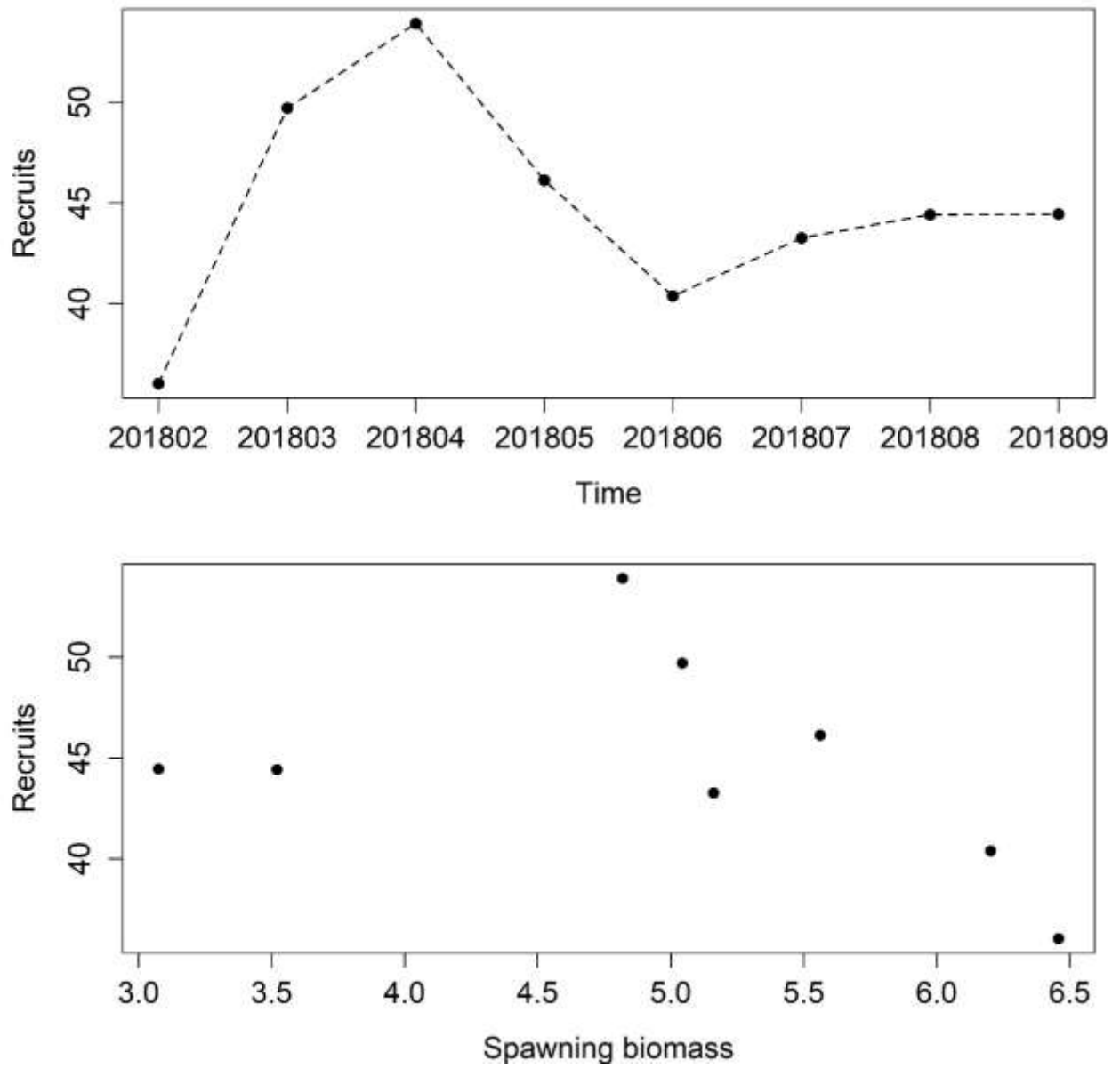


Figure 16. The estimates of recruitments (upper panel) from sensitivity scenario 1 and the relationship between spawning biomass and recruitments (lower panel)

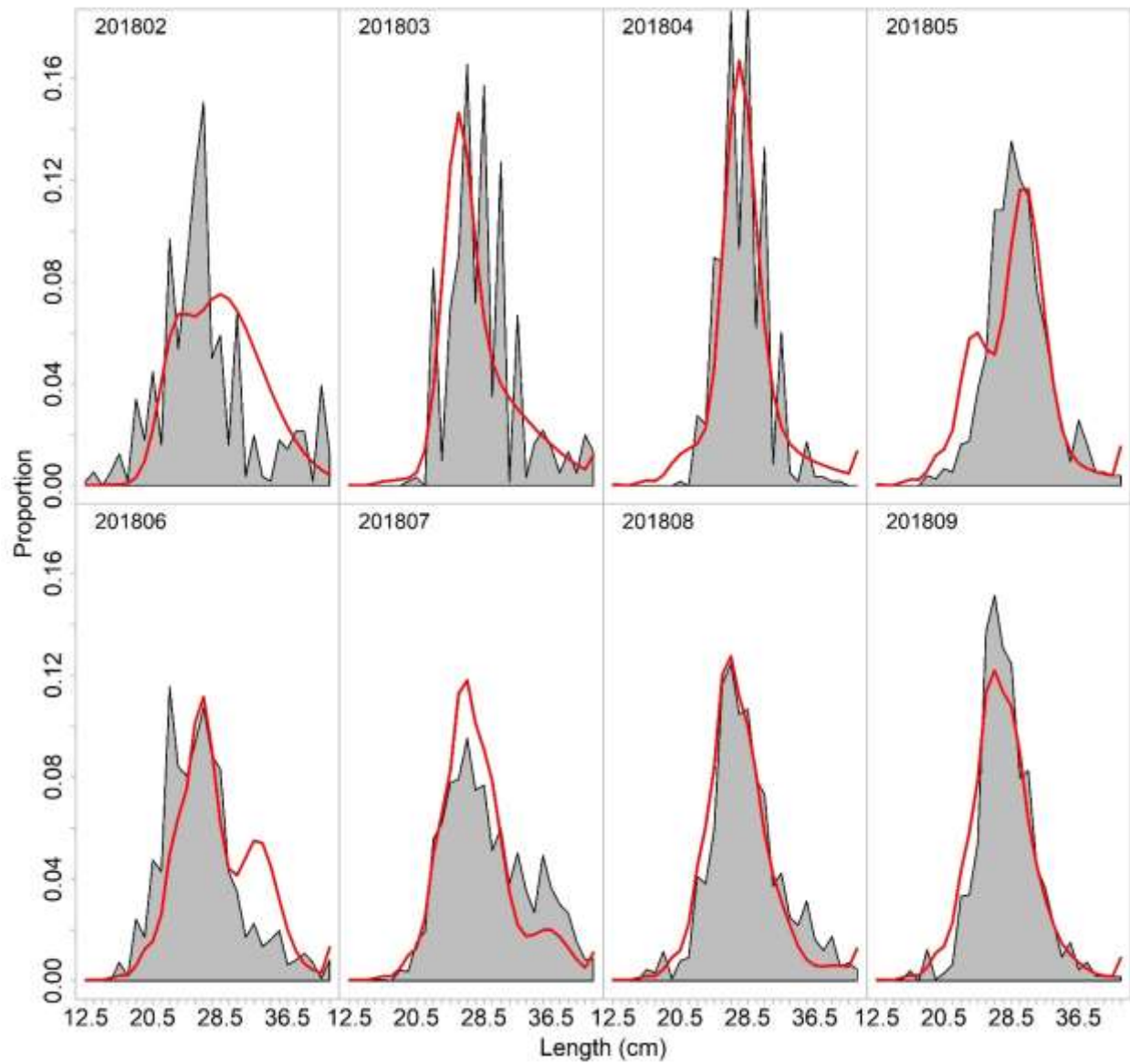


Figure 17. The observed size composition data and the predicted size compositions from sensitivity scenario 1; the red line represents the prediction

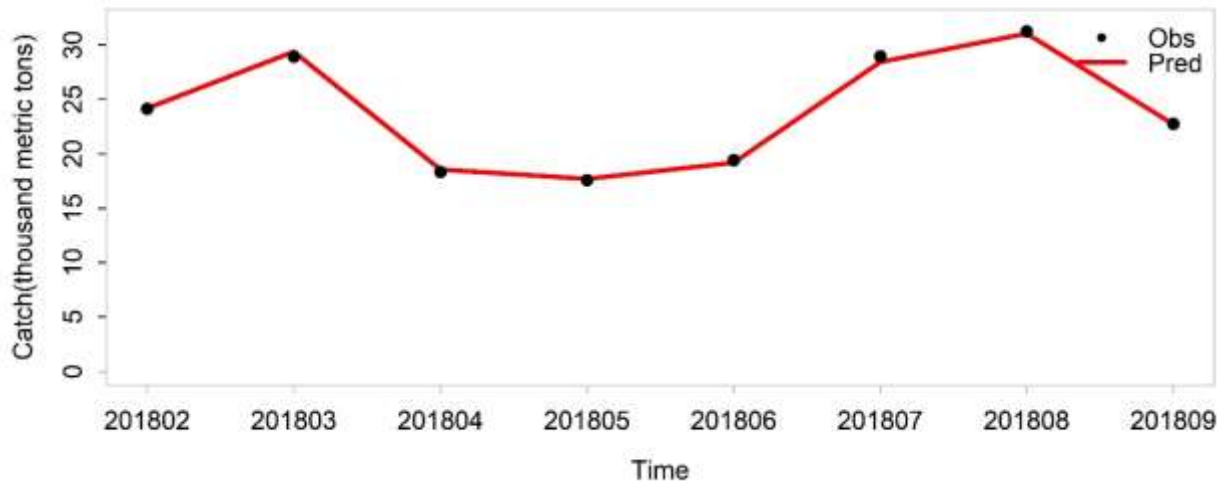
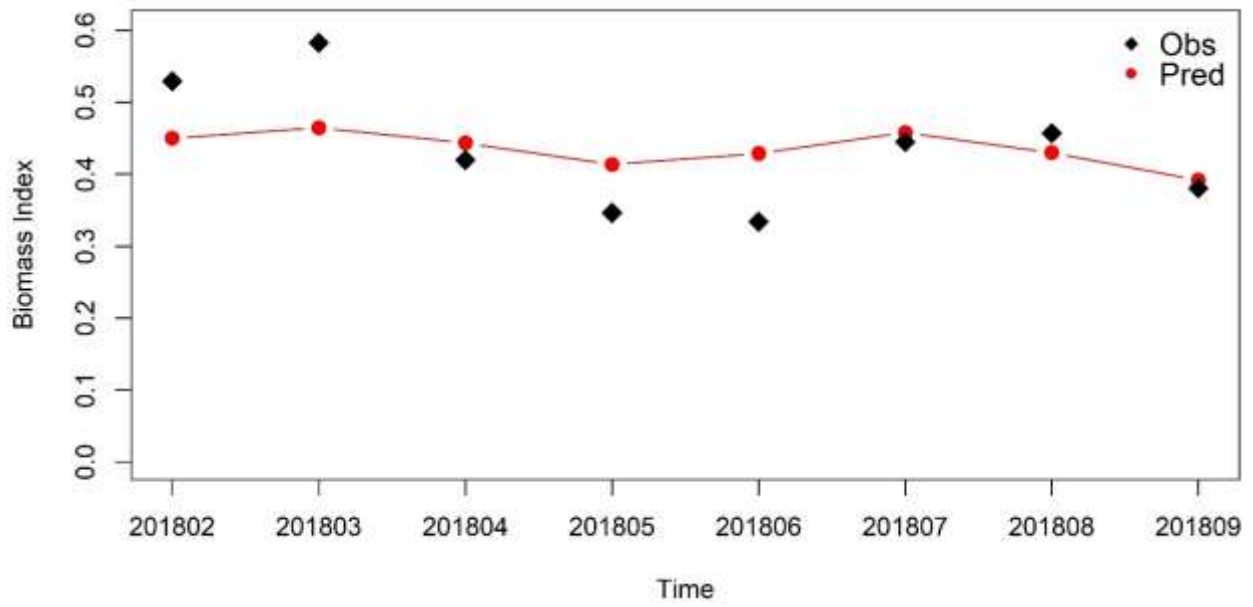


Figure 18. The observed and the predicted biomass index (upper panel) and catch (lower panel); the red line represents the prediction

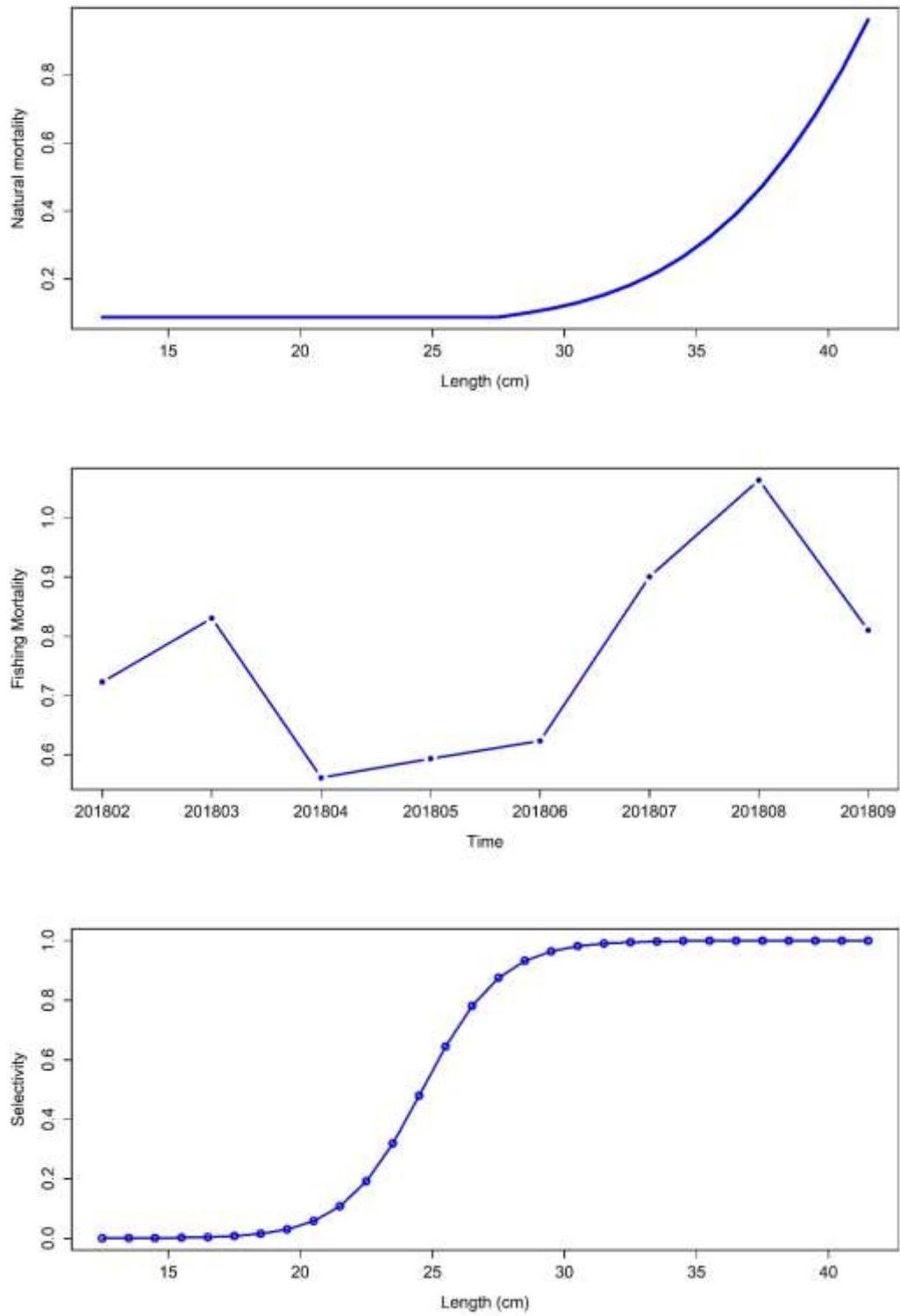


Figure 19. The estimates of natural mortality (upper panel), fishing mortality (middle panel), and selectivity (lower panel) from sensitivity scenario 2

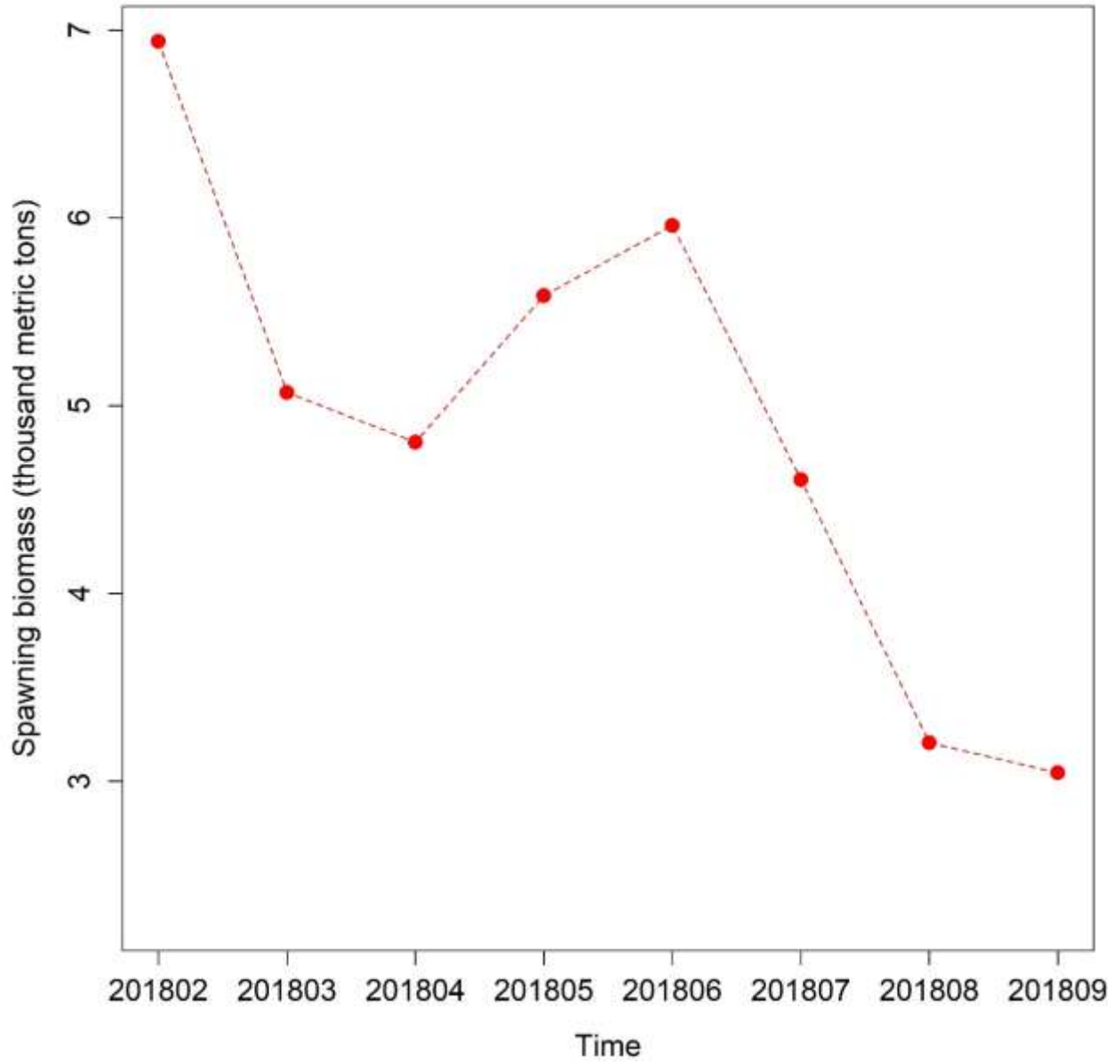


Figure 20. The estimates of spawning biomass from sensitivity scenario 2

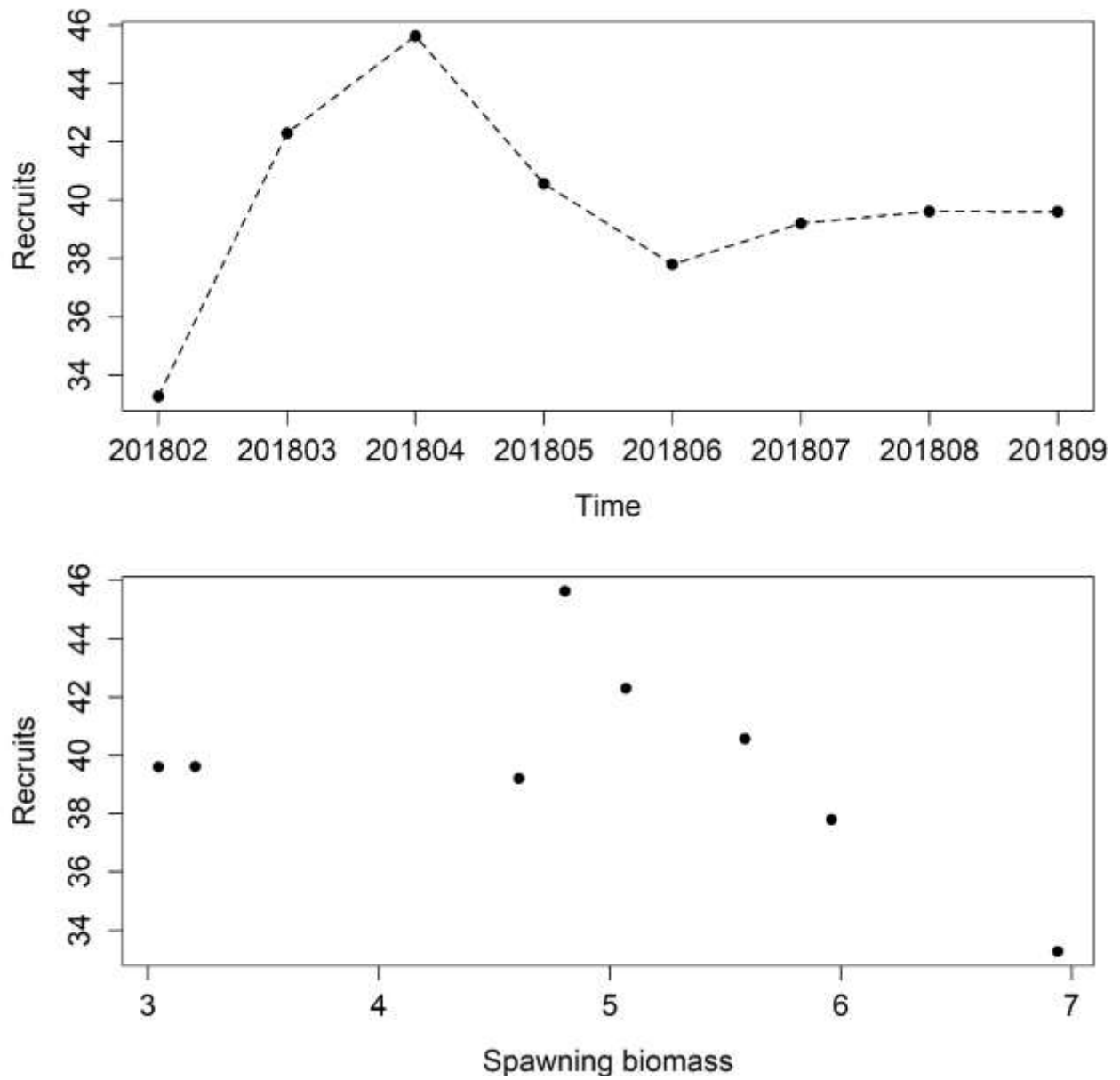


Figure 21. The estimates of recruitments (upper panel) from sensitivity scenario 2 and the relationship between spawning biomass and recruitments (lower panel)

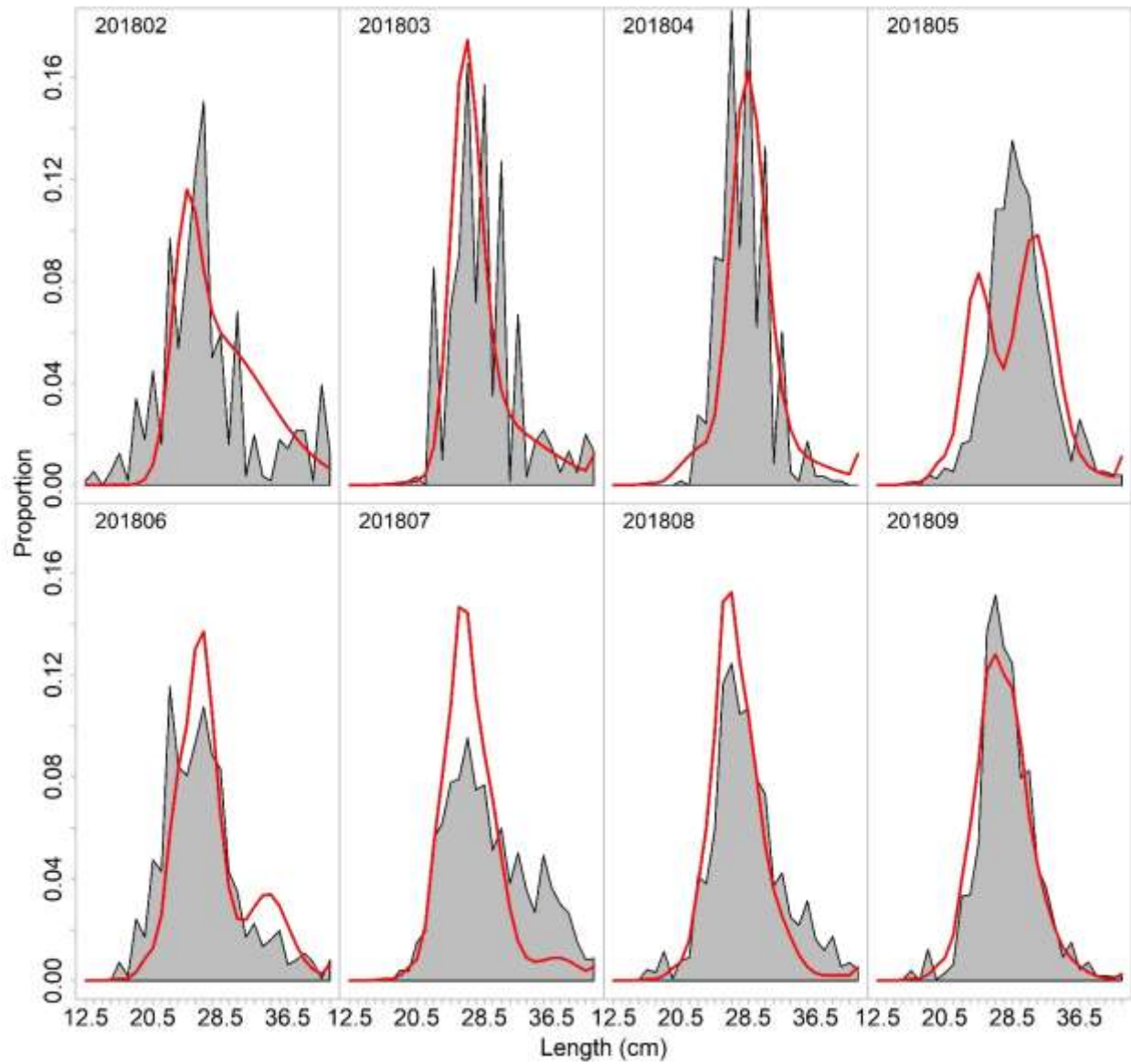


Figure 22. The observed size composition data and the predicted size compositions from sensitivity scenario 2; the red line represents the prediction

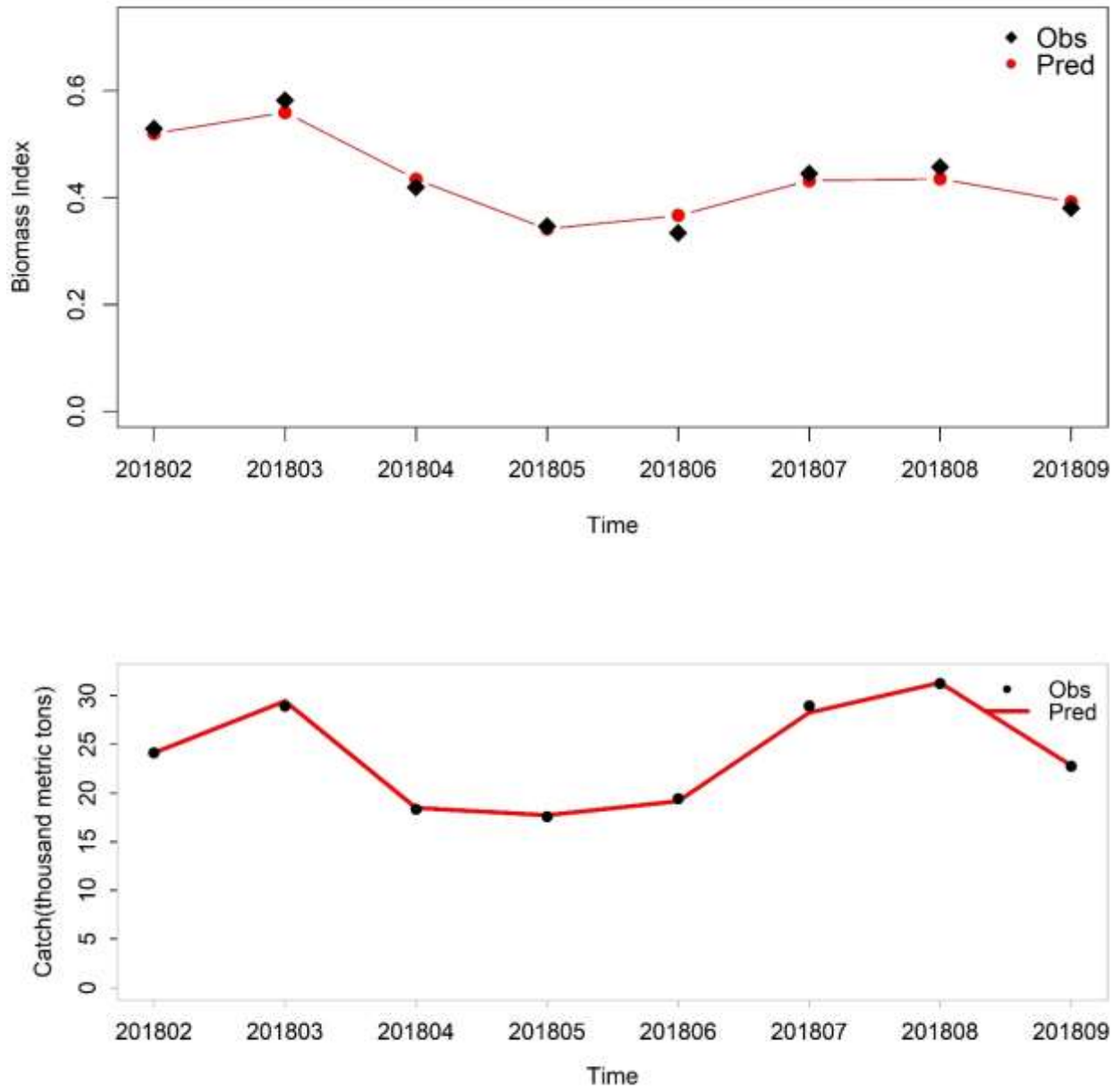


Figure 23. The observed and the predicted biomass index (upper panel) and catch (lower panel); the red line represents the prediction

References:

- Arkhipkin, A., Argüelles, J., Shcherbich, Z., Yamashiro, C., 2015. Ambient temperature influences adult size and life span in jumbo squid (*Dosidicus gigas*). *Can. J. Fish. Aquat. Sci.* 72, 400–409. <https://doi.org/10.1139/cjfas-2014-0386>
- Chen, X., Li, J., Liu, B., Chen, Y., Li, G., Fang, Z., Tian, S., 2013. Age, growth and population structure of jumbo flying squid, *Dosidicus gigas*, off the Costa Rica Dome. *J. Mar. Biol. Assoc. United Kingdom* 93, 567–573. <https://doi.org/10.1017/S0025315412000422>
- Francis, R.I.C.C., 2011. Data weighting in statistical fisheries stock assessment models. *Can. J. Fish. Aquat. Sci.* 68, 1124–1138. <https://doi.org/10.1139/f2011-025>
- Haddon, M. (2010). *Modelling and quantitative methods in fisheries*. CRC press.
- Liu, B., Chen, X., Chen, Y., Tian, S., Li, J., Fang, Z., Yang, M., 2013. Age, maturation, and population structure of the Humboldt squid *Dosidicus gigas* off the Peruvian Exclusive Economic Zones. *Chinese J. Oceanol. Limnol.* 31, 81–91. <https://doi.org/10.1007/s00343-013-2036-z>
- SPRFMO, 2018. A size-structured model for jumbo squid in south-east Pacific. Available on <https://www.sprfmo.int/assets/2018-SC6/Meeting-Documents/SC6-SQ06-China-Size-structure-model-squid.pdf>